THE JOURNAL OF BIOLOGICAL CHEMISTRY VOL. 287, NO. 40, pp. 33512–33522, September 28, 2012

Expression of the Hutchinson-Gilford Progeria Mutation during Osteoblast Development Results in Loss of Osteocytes, Irregular Mineralization, and Poor Biomechanical Properties*[S]

Received for publication, March 27, 2012, and in revised form, July 26, 2012 Published, JBC Papers in Press, August 14, 2012, DOI 10.1074/jbc.M112.366450

Eva Schmidt[‡1], **Ola Nilsson**[§2], **Antti Koskela**[¶], **Juha Tuukkanen**[¶], **Claes Ohlsson**[‖], **Björn Rozell**[**], **and Maria Eriksson**[‡3]

From the [‡]*Department of Biosciences and Nutrition, Center for Biosciences, Karolinska Institutet, Huddinge SE-14183, Sweden, the* [§]*Department of Women's and Children's Health, Karolinska Institutet and University Hospital, Solna, Stockholm SE-17177, Sweden, the* [¶]*Department of Anatomy and Cell Biology, University of Oulu, Oulu FI-90014, Finland, the* [‖]*Department of Internal Medicine, Sahlgrenska Academy, University of Gothenburg, Gothenburg SE-40530, Sweden, and the* [**]*Department of Veterinary Disease Biology, Faculty of Health and Medical Sciences, University of Copenhagen, Copenhagen DK-1165, Denmark*

Background: Tissue-specific mouse model for Hutchinson-Gilford progeria syndrome (HGPS).
Results: Dysfunctional osteoblast maturation and impacts DNA damage and Wnt signaling, which lead to abnormal bone mineralization and impaired skeletal and dental structures.
Conclusion: Resemble clinical features of HGPS and normal bone aging.
Significance: Provides insights to the molecular mechanisms of HGPS and will be useful to further elucidate the processes that contribute to general bone aging.

Hutchinson-Gilford progeria syndrome (HGPS) is a very rare genetic disorder that is characterized by multiple features of premature aging and largely affects tissues of mesenchymal origin. In this study, we describe the development of a tissue-specific mouse model that overexpresses the most common HGPS mutation (*LMNA*, c.1824C>T, p.G608G) in osteoblasts. Already at the age of 5 weeks, HGPS mutant mice show growth retardation, imbalanced gait and spontaneous fractures. Histopathological examination revealed an irregular bone structure, characterized by widespread loss of osteocytes, defects in mineralization, and a hypocellular red bone marrow. Computerized tomography analysis demonstrated impaired skeletal geometry and altered bone structure. The skeletal defects, which resemble the clinical features reported for bone disease in HGPS patients, was associated with an abnormal osteoblast differentiation. The osteoblast-specific expression of the HGPS mutation increased DNA damage and affected Wnt signaling. In the teeth, irregular dentin formation, as was previously demonstrated in human progeria cases, caused severe dental abnormalities affecting the incisors. The observed phenotype also shows similarities to reported bone abnormalities in aging mice and may therefore help to uncover general principles of the aging process.

Hutchinson-Gilford Progeria Syndrome (HGPS,[4] progeria, OMIM#176670) is a rare segmental progeroid genetic disorder that affects one in 4–8 million live births (1). Patients appear normal at birth, but during the first years of life, symptoms start appearing and include severe growth retardation, loss of subcutaneous adipose tissue, hair loss, atrophy, and wrinkling of the skin, micrognathia, delayed tooth eruption, formation of irregular secondary dentin obliterating the dental pulp and stiffness of joints (2, 3, 4). In addition, they show skeletal abnormalities, including abnormalities in bone morphology and alterations in bone structure, which result in a unique skeletal dysplasia (5). The majority of patients die from progressive atherosclerosis at a median age of 13 years (6, 7).

Most of the classical HGPS cases are the result of a single *de novo* point mutation within exon 11 of the *LMNA* gene (G608G, GGC>GGT) (8, 9). The *LMNA* gene codes for the A-type lamins, lamin A, AΔ10, C, and C2 (10, 11). Lamin A is synthesized first as the precursor molecule, prelamin A, which undergoes modification before it becomes mature lamin A (12, 13). The maturation of prelamin A initially requires farnesylation of the C terminus followed by cleavage of the three C-terminal amino acids, carboxymethylation of the farnesylated cysteine and finally, the cleavage of the fifteen terminal amino acids. The endoprotease, Zmpste24, is responsible for the final cleavage of the prelamin A molecule (14, 15). The most common HGPS mutation activates a cryptic splice site and results in a form of the prelamin A protein that contains an internal deletion of 50 amino acids (9). This deletion results in the removal of the rec-

* This work was supported by grants from the Karolinska Institutet, the Swedish Research Council, the Swedish Foundation for Strategic Research, the Torsten and Ragnar Söderberg Foundation, the Tore Nilsson Foundation, the Åke Wiberg Foundation, the Hagelen Foundation, and the Loo and Hans Osterman Foundation.
[S] This article contains supplemental Table S1.
[1] Supported by Karolinska Institutet KID faculty funding.
[2] Supported by ESPE research fellowship grants, the Swedish Society of Medicine, HKH Kronprinsessan Lovisas Förening for Barnasjukvård, Sällskapet Barnavård, and Stiftelsen Frimurare Barnhuset i Stockholm.
[3] To whom correspondence should be addressed: Department of Biosciences and Nutrition, Center for Biosciences, Karolinska Institutet, Novum, SE-14183 Huddinge, Sweden. Tel.: +46852481066; Fax: +46852481170; E-mail: Maria.Eriksson.2@ki.se.

[4] The abbreviations used are: HGPS, Hutchinson-Gilford progeria syndrome; tTA, tetracycline-responsive transcriptional activator; BMD, bone mineral density; RT-PCR, reverse transcription-PCR; TRAP, tartrate-resistant acid phosphatase; pQCT, peripheral quantitative computed tomography; DAPI, 4′,6-diamidino-2-phenylindole; Alp, alkaline phosphatase; Col1a1, Collagen type 1α1; Ocn, Osteocalcin; CTSK, cathepsin K.

ognition site that is required for the final proteolytic step. The resulting farnesylated and carboxymethylated lamin A protein is designated progerin. Cells expressing progerin are characterized by an abnormal shape and lobulation of the cell nucleus, loss of peripheral heterochromatin, thickening of the nuclear lamina, and clustering of nuclear pore complexes (16–18).

Mouse models previously generated to reflect bone abnormalities in progeria patients exhibit growth retardation, abnormal gait, immobility of the joints, deformations of the skeleton and changes in bone mineral density (BMD) (14, 19, 20). Homozygous *lmna*$^{HG/HG}$ mice, that express progerin exclusively and no lamin A or C, displayed severe bone abnormalities, including spontaneous bone fractures in the extremities, poorly mineralized bones and premature death (21). In addition to skeletal abnormalities, Zmpste24-deficient mice also showed malformation of the teeth (15, 22).

To increase the understanding of bone and dental diseases in HGPS, we have developed an inducible and tissue-specific mouse model, which expresses the most common HGPS mutation, c.1824C>T, p.G608G, in osteoblasts and odontoblasts (23, 24). The previously described osterix transactivator mouse, Sp7-tTA (25, 26), was intercrossed with two different mouse lines carrying minigenes of human lamin A under the control of a pTRE element (tetop). Our results show that inducible expression of a minigene of human lamin A with the HGPS mutation during bone development in mice results in skeletal abnormalities, characterized by irregular cortical bone with poor biomechanical properties and widespread loss of osteocytes and osteoblasts. These changes are associated with impaired osteoblast differentiation, decline in DNA damage signaling and altered Wnt signaling. Our findings demonstrate that this mouse model exhibit a bone disease similar to that of HGPS and may thus be useful for increasing the understanding of lamin A in dystrophic osteogenesis as well as during aging. In addition, this model is, to our knowledge, the only available model with inducible and tissue-specific expression of the HGPS mutation in the bone and will be useful for testing treatments for HGPS.

EXPERIMENTAL PROCEDURES

Animal Housing—Animals were housed in a 12 h light/dark cycle, at temperatures of 19–23 °C and 50–65% air humidity at the animal facility at the Karolinska University Hospital, Huddinge, Sweden. The animals were fed autoclaved RM3(P) pellets (Scanbur, Sweden), and drinking water was provided *ad libitum*. All animal studies were approved by the Stockholm South Ethical review board, Dnr. S141-06 and S107-09.

Generation of Binary Transgenic Mice—We obtained B6.Cg-Tg (Sp7-tTA, tetO-EGFP/cre)1Amc/J promoter mice (referred to as Sp7-tTA) from The Jackson Laboratory, stock number: 006361. Sp7-tTA mice were maintained by mating to C57BL/6J, and 100 μg/ml doxycycline/2.5% sucrose was included in the drinking water according to suggestions from the donating investigator. To target HGPS transgenic expression to bone tissue, FVB/N-Tg (tetO-LMNA*G608G,-EGFP) VF1–07Maer (referred to as tetop-LA^{G606G}), and FVB/N-Tg (tetO-LMNA,-EGFP) SF1–04Maer (referred to as tetop-LA^{wt}) mice (24) were intercrossed with the Sp7-tTA transgenic mice. All animals were genotyped according to published protocols (24, 25). The bitransgenic offspring, tetop-LA^{G608G+}; Sp7-tTA^{+}, are referred to as HGPS mice. The bitransgenic offspring, tetop-LA^{wt+}; Sp7-tTA^{+}, are referred to as human LA mice. The single transgenic offspring, tetop-LA^{G608G+}; Sp7-tTA^{-} and tetop-LA^{wt+}; Sp7-tTA^{-}, are referred to as control mice. The non-transgenic offspring, tetop-LA^{G608G-}; Sp7-tTA^{-}, are referred to as wild-type mice. The offspring that resulted from the intercross breeding were provided with softened/moist food pellets (see above) on the cage floor after weaning. The weight of the animals was recorded every week from postnatal week 2. Animals were sacrificed with an overdose of Isofluran (Baxter, Sweden) at postnatal week 5 and 12, and tissues (femur, tibia, spine, skull, lower jaw, skin, heart, liver, spleen, kidney, testis, ovaries, and limb muscle) were collected. X-ray images were taken from animals at the age of 12 weeks using a Mobilett x-ray unit (Siemens).

Extraction of Total RNA and Protein from Bone—The tibia was collected, and the epiphyses were cut off. The bone marrow cavity was flushed with PBS using a 27-gauge needle. The empty bone was immediately transferred to liquid nitrogen. The tissue was homogenized using a Bessmann tissue homogenizer and transferred to Matrix Lysing D (Qbiogene) containing either TriZol® (Invitrogen) for RNA extraction or 8 M urea/RIPA buffer (including proteinase inhibitors, Roche) for protein extraction. For further homogenization, the Fastprep 220A (Qbiogene) was used twice at 6 ms^{-1} for 40 s. Samples were incubated on ice for 10 min between each run.

Analysis of Transgenic Expression—The analysis of transgenic expression on RNA levels was performed in bone, cartilage, brain, skeletal muscle, heart, liver, and fat tissue for HGPS (n = 3) and control mice (n = 4). RNA was isolated from 12-week-old mice using the TriZol® reagent (Invitrogen). The cartilage was microdissected from 5-day-old pups and the RNA was extracted with proteinase K (20 mg/ml), 4 M guanidine thiocyanate, 25 mM sodium citrate, pH 7.0, and 0.1 M β-mercaptoethanol (27). Random hexamers and SuperScript II Reverse Transcriptase (Invitrogen) were used to synthesize cDNA from 1 μg of RNA. A transgene-specific assay was performed for the lamin A minigenes according to the previously published procedure (24). RT-PCR analysis with β-actin specific primers (28) was performed on all samples as a control. Enhanced protein separation and Western blot analysis was performed as previously described (24). The primary antibodies used for Western blot included mouse monoclonal anti-human lamin A+C (mab3211, Chemicon), goat polyclonal anti-lamin A/C (sc-6215, Santa Cruz Biotechnology) and mouse monoclonal anti-β-actin (A5441, Sigma). Densitometry was performed using the Versa Doc Imaging System, and the results were analyzed with Quantity One software (Bio-Rad).

Histology—The skeletal preparations of the fore limbs were performed according to Nagy *et al.* (29). The tissues were fixed overnight in 4% paraformaldehyde, pH 7.4. Decalcification of the lower jaw, femur, and skull was performed in 12.5% EDTA for 5 days and the spine for 10 days and thereafter processed for dehydration and embedded in paraffin wax. 4-μm Sections were stained with Hematoxylin & Eosin, and a combination of Alcian Blue, pH 2.5, and Van-Gieson. The osteoclasts were

visualized using a histochemical staining kit to detect tartrate-resistant acid phosphatase (TRAP) according to the manufacturer's instructions (Kit 387A, Sigma).

Histomorphometry—The osteocyte lacunae differential count was performed on 4-μm femoral sections stained with Hematoxylin & Eosin using a bright light microscope. A total number of 300 lacunae was counted in identical areas of the diaphysial cortical bone from HGPS ($n = 3$) and control mice ($n = 3$). Osteocyte lacunae were further distinguished in lacunae containing live cells, with osteocytes showing well-defined and well-preserved nuclei, and empty lacunae, containing no nuclei or a degenerated cell. The cell counts were normalized for the total number of counted lacunae.

Bone Quality Analysis—To assess the bone quality, we collected long bones (tibia and femur) from male and female HGPS and control mice ($n = 6$, respectively) at the age of 12 weeks. After fixation in 4% paraformaldehyde, the bones were transferred to 70% EtOH and processed for peripheral quantitative computed tomography (pQCT) and the three-point bending test. The computed tomographic scans were performed with the pQCT XCT RESEARCH M system (Version 4.5B, Norland, Fort Atkinson, WI) operating at a resolution of 70 μm, as described previously (30). The trabecular volumetric BMD (vBMD) was determined with a metaphyseal pQCT scan of the long bones. The scan was positioned at the metaphysis at a distance that was distal from the proximal growth plate corresponding to 3% of the total length of the bone, and the trabecular bone region was defined as the inner 45% of the total cross-sectional area. The cortical bone parameters (cortical vBMD and cortical thickness) were analyzed in the mid-diaphyseal region of the bone. The biomechanical properties of the bones were analyzed by the three-point bending test, with a span length of 5.5 mm and a loading speed 0.155 mm/min, and was performed for tibial and femoral diaphysis, while axial loading was performed for the femoral neck using the Instron universal testing machine (Instron 3366, Instron Corp., Norwood, MA). Previously developed principles of bone biomechanical testing were applied (31, 32). The biomechanical parameters were calculated based on the recorded load deformation curves.

Quantitative RT-PCR Analysis—The real-time PCR reactions were performed in 20-μl reaction volumes containing 5 μl of diluted cDNA template in MicroAmp 96-well plates sealed with optical adhesive covers (Applied Biosystems). Each experiment contained cDNA or a no template control, 1× Power SYBR® Green and 0.2 pmol/μl of the respective forward and reverse primer. The primer sequences are provided in supplemental Table S1. After the plates were prepared, they were loaded onto an ABI7500 fast system sequencing detection instrument and run with the following cycling conditions: 2 min at 50 °C, 10 min at 95 °C, then 40 cycles each of 15 s at 95 °C and 40 s at 60 °C. All reactions were run in triplicate, and each sample group had an $n = 3$. The variation among the triplicates of ≤0.3 units for C_T values below 30 and ≤0.5 units for C_T values above 30 was considered acceptable. To calculate the relative changes in gene expression, the $2^{-\Delta\Delta C}{}_T$ comparative C_T method was used (33). The data were interpreted as the expression of the gene of interest relative to the reference gene (β-actin) in HGPS mice compared with wild-type animals.

Primary Osteoblast Cultures—Animals at the age of postnatal day 5 and 12 weeks were euthanized with an overdose of Isofluran (Baxter, Sweden). Primary osteoblasts were extracted according to the previously published procedure (34) and were processed for the *in vitro* mineralization assay and cytospin staining.

In Vitro Mineralization Assay—Cells were plated at 25,000 cells/cm^2 in 12-well plates, grown to confluence in αMEM/10% FBS with antibiotics, and differentiated in osteoblast culture media containing 100 μg/ml ascorbate and 5 mM β-glycerophosphate. For histochemical assessment of alkaline phosphatase (Alp) activity, osteoblast cultures were fixed in 4% paraformaldehyde and stained for 20 min with a solution containing 0.1 mg/ml naphthol AS-MX phosphate and 0.6 mg/ml Fast blue BB salt (Sigma-Aldrich). To stain for calcium deposition, cultures were fixed in 4% paraformaldehyde, stained for 30 min with 0.1% Alizarin Red at pH 5.5, and rinsed several times with deionized water to remove nonspecifically bound stain. Alp-, and Alizarin Red-stained osteoblast cultures were analyzed using an Axiovert Zeiss microscope. Three 12-well plates per sample were analyzed in each experiment. The staining intensity was evaluated by three independent researchers using a 4 unit scoring system. The criteria for scoring the degree of staining ranged from 1 (no staining) to 4 (intense staining).

Cytospin—1×10^3 cells were washed with 200 μl of PBS, centrifuged at 0.2 rcf for 10 min and resuspended in 200 μl of PBS. The cells were centrifuged onto SuperFrost Plus glasses (Menzel, Germany) with Thermo Shandon filter cards using the Shandon Cytospin 4 machine at medium acceleration rate, 500 rpm for 15 min.

Immunofluorescence—Cytospins were fixed with 4% paraformaldehyde, permeabilized with 1% Nonidet P-40 detergent (Pierce) in PBS and blocked with 5% goat serum/0.1% Birj (Pierce) in PBS (13). All incubations were performed using a MIST tray. The primary antibodies used were a rabbit polyclonal anti-mouse collagen type 1 (BT21–5014, Biotrend) co-stained with a mouse monoclonal anti-human lamin A+C antibody (mab3211, Chemicon) or a mouse monoclonal anti-phospho-Histone H2A.X (γH2AX) (JBW301, Millipore). The cells were incubated with 4′,6-diamidino-2-phenylindole (DAPI) at the concentration of 0.1 mg/ml prior to mounting using the ProLong® Gold antifade reagent (Invitrogen). The frequency of cytoplasmic collagen type 1 stained cells with nuclear human lamin A/C staining was calculated from isolated osteoblasts of HGPS mice ($n = 5$) and control mice ($n = 4$). The fraction of cells that was positive for cytoplasmic collagen type 1 staining was analyzed for presence of γH2AX foci. The fraction of cytoplasmic collagen type 1 positive cells with ≥5 γH2AX foci was counted from HGPS mice ($n = 3$) and wild-type mice ($n = 3$). A minimum of 300 cytoplasmic collagen type 1-stained cells was counted for each animal.

Statistical Analysis—The unpaired Student's *t* test was used for data analysis. Values represent the mean ± S.E. *p* values of <0.05 were considered significant (*, $p < 0.05$; *P*, **<0.01; *P*,***< 0.001).

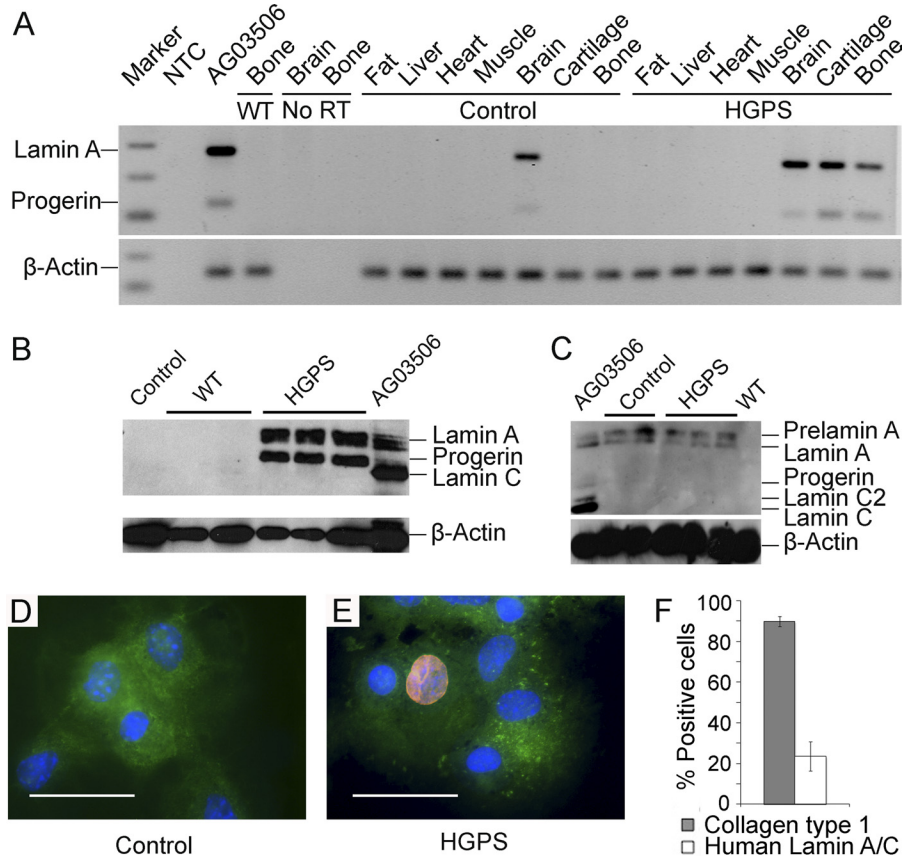

FIGURE 1. **Transgenic expression in the bone is regulated by the transactivator.** The transgenic expression of human lamin A and progerin detected in RNA (*A*) and protein extracts (*B* and *C*) from HGPS mice and a human HGPS control sample (AG03506). The tissues analyzed for the transgenic expression of RNA levels included bone, cartilage, brain, skeletal muscle, heart, liver, and fat. A no RT-control for bone and brain and a no-template-control (*NTC*) were included in the PCR reactions (*A*). There was no detectable expression in control or wild-type (*WT*) samples of RNA (*A*) or protein (*B*) in the bone. In the brain protein samples from HGPS mice and control mice, expression of prelamin A and lamin A, but no progerin expression was detected (*C*). The human-specific lamin A/C antibody (*red*) detects transgenic expression of human lamin A and progerin in primary osteoblasts isolated from HGPS mice (*E*). No lamina staining was detected in osteoblasts from control mice. Collagen type 1 antibody (*green*) was used as an osteoblast marker), and nuclei were counterstained with DAPI (*blue*) (*D*). The quantification of cells from the calvariae explant cultures showed that 89.7 ± S.E. 2.5% of all isolated cells are collagen type 1-positive, of which 23.6 ± S.E. 7.1% stained positive for human lamin A/C (*F*). Scale bars: 50 μm.

RESULTS

The Transactivator Regulates the Transgenic Expression—The lamin A transgenic mice, tetop-LA^{G608G} and tetop-LA^{wt}, were intercrossed with the Sp7-tTA promoter, and the transgene expression was analyzed by RT-PCR (Fig. 1*A*), Western blot (Fig. 1, *B* and *C*), and immunofluorescence (Fig. 1, *D* and *E*). The amplification of human lamin A and lamin Adel150 (progerin) was detected in bone, cartilage, and brain tissue isolated from HGPS mice after the cDNA had undergone 35 PCR cycles. Although the amplification products were also detected in the brain of control mice, transgenic expression was not observed in the bone or cartilage of control mice, indicating that the transgenic expression was regulated by the transactivator in these tissues (Fig. 1*A*). Western blot analysis with an antibody specific for human lamin A/C revealed transgenic expression of lamin A and progerin in bone protein extracts from HGPS mice, whereas bone protein extracts from human LA mice only showed lamin A expression (Fig. 1*B*, and data not shown). No transgenic expression was seen in the protein extracts from the bones of control mice, demonstrating that activation is dependent on the transactivator (Fig. 1*B*). In protein extracts from the brain, human lamin A was detected in both HGPS and control mice, indicating that the tetop-LA^{G606G} minigene was at least partially being expressed in the brain and even in the absence of the transactivator (Fig. 1*C*). The relative expression levels of the minigene compared with expression of mouse lamin A were quantified using densitometry on western filters that were hybridized with an antibody that recognized lamin A/C of mouse and human origin (data not shown). In HGPS mice (n = 3), the average expression ratio of human lamin A and progerin compared with mouse lamin A was 1.03, which indicates that the average transgenic overexpression was close to 100%.

Immunofluorescence with the human lamin A/C specific antibody, mab3211, on cytospins showed no staining in control mice (n = 4) (Fig. 1*D*) whereas distinct lamina staining was detected in cells isolated from HGPS mice (n = 5) at the age of 5 weeks (Fig. 1*E*). This showed that the antibody is very useful to detect the transgenic expression of human lamin A and progerin since it does not cross-react with the mouse lamin A/C. To test our extraction method of osteoblasts from the calvariae, we used a Collagen type 1 antibody as an osteoblast expressed marker to calculate the frequency of collagen type 1 positive cells in the calvariae explant cultures. Our results showed that, on average, 89.7 ± S.E. 2.5% of all isolated cells expressed Col-

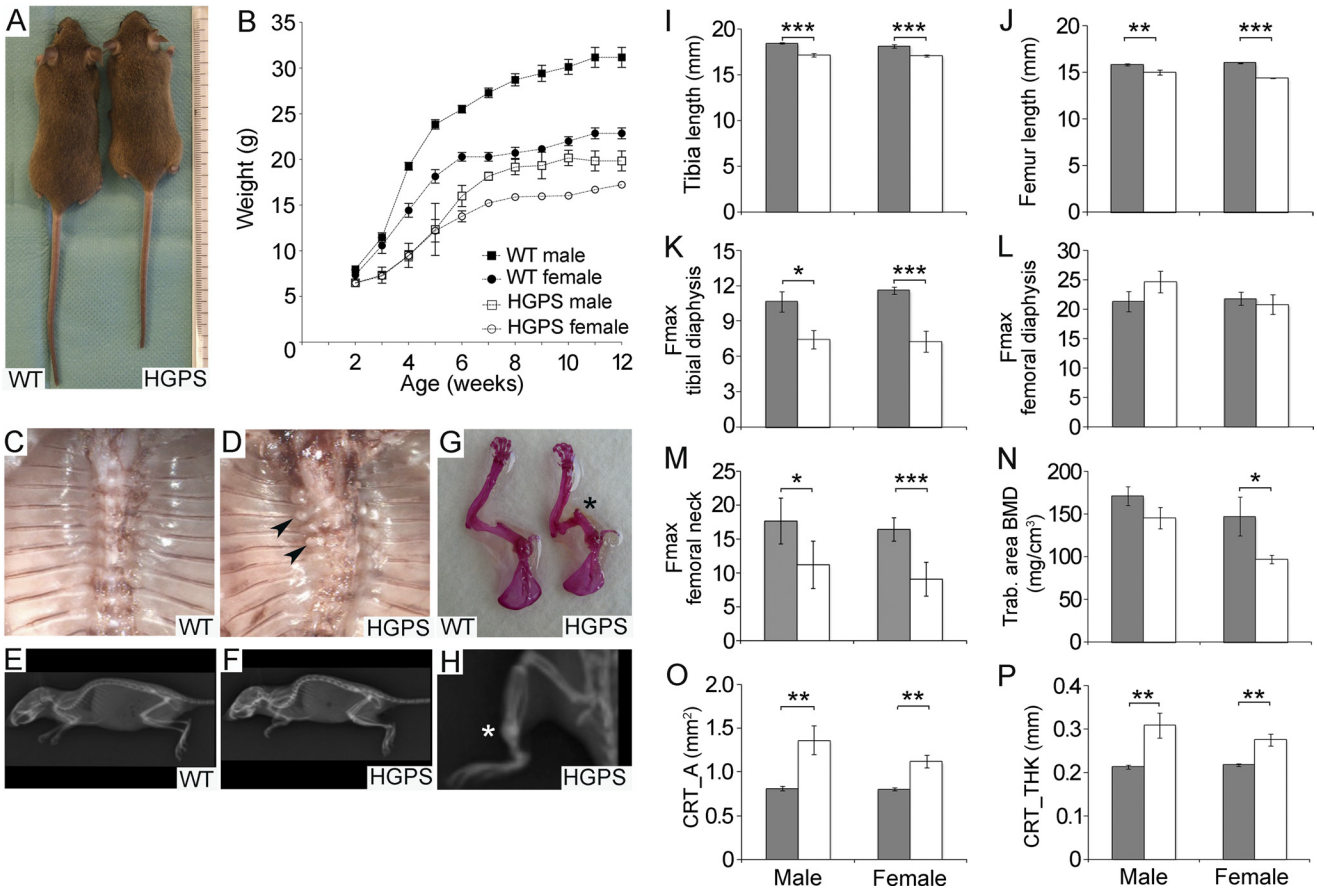

FIGURE 2. **The expression of the HGPS mutation in osteoblasts results in growth retardation, bone fractures, and altered bone quality.** Photograph and radiograph images of 12-week-old HGPS mice (*A* and *F*) *versus* wild-type littermate mice (*A* and *E*). The HGPS mice ($n = 16$) showed reduced growth rates compared with wild-type mice ($n = 19$) (*B*). The thorax of 12-week-old wild-type (*C*) and HGPS mice (*D*). Fractures and callus formation were detected close to the costovertebral junction in HGPS mice (*D*, *arrowheads*), but not in wild-type animals (*C*). Skeletal abnormalities, such as scoliosis (*D*) and kyphosis (*F*) were noted in the HGPS mice only. Fractures (*asterisk*) were detected in Alizarin Red skeletal preparations in humerus (*G*) and in the tibia on radiograph images (*H*) in HGPS mice. Shorter bones were seen in HGPS mice compared with control mice when bone length was measured in tibia (*I*) and femur (*J*) from male and female HGPS and control mice. Impaired skeletal integrity and compromised bone strength (Fmax, maximum load at bone failure) were detected in tibial diaphysis (*K*) and femoral neck (*M*) from HGPS mice by three-point bending test but femoral diaphysis was not significantly affected (*L*). Reduced values for trabecular bone mineral density (BMD) (*N*), and increased measurements for the cortical bone area (*O*) and thickness (*P*) in male and female HGPS mice. *Solid gray bars*, WT; *empty bars*, HGPS. All values represent measurements of the mean ± S.E. (*, $p < 0.05$, **, $p < 0.01$, ***, $p < 0.001$).

lagen type I ($n = 4$). The frequency of cells isolated from HGPS mice that were positive for transgenic expression was 23.6 ± S.E. 7.1% ($n = 5$) (Fig. 1*F*).

External Phenotypes—The HGPS mice were indistinguishable from littermate controls at birth through the weaning of the litters at postnatal day 21. However, during their fourth postnatal week, the weight dropped, possibly due to dental abnormalities. Incisors that were bent outwards and broken were observed in the HGPS mice, and all mice were provided with a soft diet on the cage floor from the day of weaning. Even when using this special diet, HGPS mice (male $n = 6$, female $n = 10$) were smaller in size (Fig. 2*A*) and had lower body weights (Fig. 2*B*) when compared with wild-type littermates (male $n = 9$, female $n = 10$).

In parallel with the observed growth retardation, at postnatal week 5, the HGPS mice ($n = 16$) displayed a wobbling gait. All HGPS mice continuously had problems standing on their hind legs and fell to the side when walking in the cage. Callus formation, which indicated fractures of the ribs close to the costovertebral junction, was not detected in wild-type and control mice (Fig. 2*C*), whereas HGPS animals displayed callus formations from postnatal week 5 (Fig. 2*D*). No skeletal deformations of the spine was detected in wild-type (Fig. 2*E*) and control mice. In HGPS mice kyphosis was apparent at the age of 12 weeks (Fig. 2*F*). With increasing age, the wobbling gait became more severe, and HGPS mice also showed kyphoscoliosis (Fig. 2*D*). The increased incidence of spontaneous fractures in long bones, accompanied by callus formation, was another striking skeletal abnormality that was only seen in HGPS mice (Fig. 2, *G* and *H*). Despite the described skeletal and dental abnormalities, the mice were viable, and no premature death was observed, with a survival up to 24 months (data not shown). At postnatal week 12, tibia and femur lengths were significantly reduced for both male (femur $p < 0.01$, tibia $p < 0.001$) and female (femur $p < 0.001$, tibia $p < 0.001$) mice, when compared with control animals of the same age (Fig. 2, *I* and *J*).

Impaired Bone Quality in HGPS Mice—To assess the biomechanical properties of the bones, three-point bending tests were performed on the tibia and femur. Reductions in the Fmax (maximum load at bone failure) indicated compromised bone strength for the measurements of tibial diaphysis as well as femoral neck from HGPS mice when compared with control

mice (Fig. 2, *K* and *M*). Instead, femoral diaphysis was not significantly affected (Fig. 2*L*). The cortical and trabecular bone structure was assessed in the femur and tibiae of 13-week-old animals using pQCT. In HGPS mice, there was an increased cortical bone area (Fig. 2*O*) and an increased cortical bone thickness (Fig. 2*P*) compared with wild-type mice. In contrast, trabecular BMD was decreased in female HGPS mice (Fig. 2*N*). The combination of an increased cortical thickness and a significant decrease in the biomechanical properties of the bone suggests a reduction in the bone tissue quality.

Bone and Dental Phenotypes in HGPS Mice—Histopathologic analysis revealed that postnatal overexpression of the HGPS mutation in osteoblasts and osteocytes has dramatic effects on the structure of the bone. In the cortical bone (long bones, spine, rib cage, skull, lower jaw) of 5-week-old HGPS mice, there was a striking loss of lamellar structure, and an increase of non-remodeled, non-mineralized matrix embedded in the cortical bone structure, as well as an significant increase ($p < 0.001$) of empty osteocyte lacunae lacking viable osteocytes ($n = 4$) when compared with wild-type mice (Fig. 3, *A*–*G*, and Fig. 4*E* and data not shown). The bone marrow cavity of HGPS mice was hypocellular, with prominent adipocytes (Fig. 3, *B* and *I*). Histologic analysis also showed callus formation at the junction between the ribs and the vertebrate bodies, likely due to early, spontaneous fractures. Although the bone structure appeared severely affected with signs of fracture sites in the ribs, no signs of inflammatory reactions were detected. We did not detect any morphologic abnormalities of articular or growth plate cartilage in any of the examined bone tissue from the HGPS mice. To ensure that the observed phenotype was not caused by overexpression of human lamin A, we also analyzed mice overexpressing a wild-type human lamin A minigene (human LA mice). These mice did not exhibit the abnormalities in the bone or dental tissues that were detected in the HGPS mice ($n = 4$), and they were indistinguishable from control mice ($n = 4$) and wild-type littermates ($n = 4$) (Fig. 3, *A* and *C*, and *E*, and *H* and data not shown).

No abnormalities were seen in the incisors and molars of any of the control mice ($n = 4$) (Fig. 4, *A* and *D*). Analysis of the HGPS incisors revealed broken incisors with tooth fragments remaining in the periodontal space and the presence of secondary inflammatory reactions around the fracture sites ($n = 4$). In addition, irregular dentine formation, with a clear demarcation line between normal primary and abnormal secondary dentine, was observed. In addition to abnormal secondary dentin structures, a polarization defect in the underlying odontoblast layer was noted. The odontoblasts at the incisal part had lost their polarization resulting in secondary dentine that was less organized toward the incisal part of the incisor (Fig. 4*B*) while the odontoblasts and the predentine layer showed a normal organization in the apical part of the incisor (Fig. 4*C*). A few apoptotic bodies were visible among the odontoblasts. We also found massive formation of irregular dentine formation obliterating the pulpal cavity of the molar teeth of HGPS mice (Fig. 4*E*).

Defective Osteoblast Differentiation and Down-regulation of Bone Biomarkers in HGPS Mice—Decreased TRAP staining on HGPS mice bone sections reflects reduced TRAP secretion of

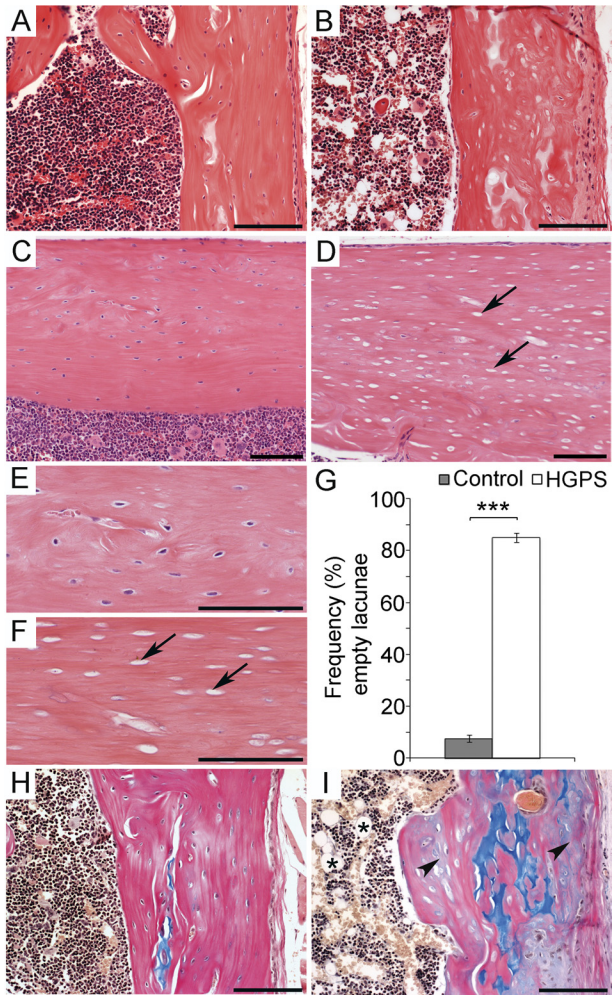

FIGURE 3. **Progerin expression during osteoblast development results in loss of osteocytes and mineralization defects.** The histological analysis of the femur of wild-type (*A*, *C*, *E*, and *H*) and HGPS mice (*B*, *D*, *F*, and *I*). Hematoxylin & Eosin staining on femur sections (*A*–*F*). In sections from wild-type mice viable osteocyte cells were detectable (*C*, and enlarged in *E*) while sections from HGPS mice showed a high frequency of empty osteocyte lacunae (*arrow*) (*D*, and enlarged in *F*). Quantitative histomorphometric analysis showed a significant increase of empty osteocyte lacunae in HGPS mice 85.1 ± S.E. 1.8% compared with wild-type mice 7.4 ± S.E. 1.4% (*G*). Unmineralized matrix was detected by Alcian blue & Van Geison staining (*H*, *I*) with cartilage stained in *blue*, mineralized tissue stained *pink*, and unmineralized tissue stained *gray* (*arrowhead*). Increased adipocyte infiltration of the bone marrow space was detected in HGPS mice only (*asterisk*) (*I*). Scale bars: (*A*, *B*, *H*, *I*) 50 μm (*C*–*F*) 100 μm. Values represent the mean ± S.E. (***, $p < 0.001$).

osteoclastic cells compared with control mice (Fig. 5, *A* and *B*). To test the differentiation capacity and the bone-forming potential of primary osteoblasts isolated from calvaria of HGPS and wild-type mice, we performed an *in vitro* mineralization assay. Osteoblasts isolated from animals at postnatal day 5 did not show any differences in proliferation and differentiation potential when cultured for 3 weeks in differentiation media and stained for Rhodamine B (Fig. 5, *C*–*F*), Alizarin red (Fig. 5, *G* and *I*) and Alp (Fig. 5, *H* and *J*). Osteoblasts isolated from HGPS mice at the age of 12 weeks showed a reduced Alp activity (score 1.3 ± S.E. 0.1, $p < 0.001$), and sparsely formed calcium deposits and bone nodules (score 2.0 ± S.E. 0.2, $p < 0.001$) after 3 weeks in differentiation media (Fig. 5*L*), whereas wild-type mice scored 2.6 ± S.E. 0.2 for Alp and 3.4 ± S.E. 0.1 for Alizarin Red (calcium deposits) (Fig. 5*K*).

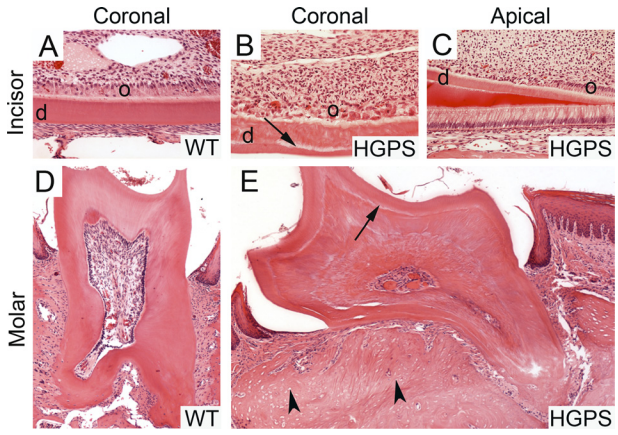

FIGURE 4. **Fractured incisors, disturbed dentine formation and abnormal odontoblast polarization in permanent and regenerative teeth.** The apical portion of the incisor (*B*) and molar roots (*E*) of HGPS mice showed a clear demarcation line (*arrow*) between primary and secondary dentine (*d*). A polarization defect in odontoblasts (*o*) that begins at the proximal part of the incisors (*C*) was detected. Both cells and secondary dentine appeared less organized toward the apical part of the teeth (*C*, and enlarged in *B*). The bone phenotype with empty osteocyte lacunae (*arrowhead*) was also present in the jaw bone of HGPS mice (*E*). No abnormalities were seen in the wild-type mice (*A*, *D*).

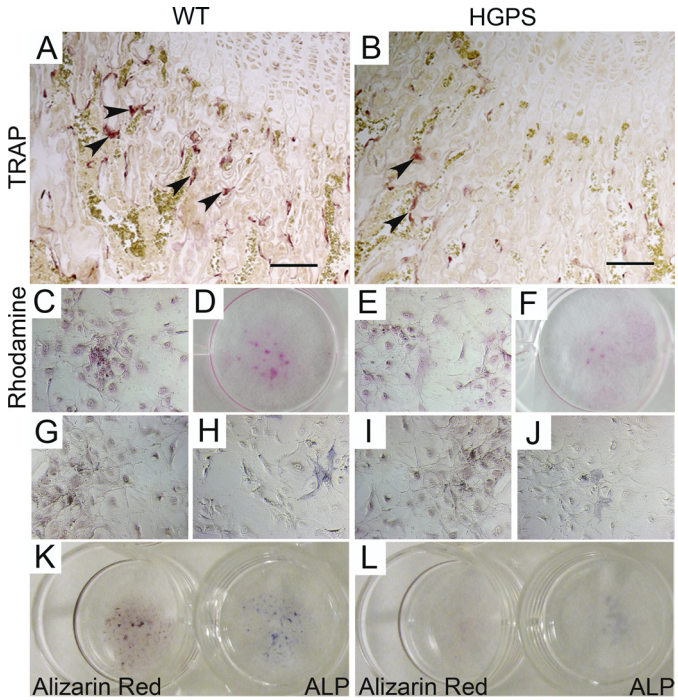

FIGURE 5. **Expression of the HGPS mutation causes a disturbed bone microenvironment and defects in bone matrix deposition.** Lower TRAP secretion, detected by enzymatic reaction for acid tartrate phosphatate on femur sections (*arrowheads*), indicates reduced osteoclast resorption activity in HGPS mice (*B*). Mineralization assay was performed on primary osteoblast cultures extracted from postnatal day 5-old-mice (*C–J*) and 12-week-old mice (*K* and *L*). Rhodamine B staining was used to check for equal cell number comparing wild-type (*C–D*) and HGPS mice (*E–F*). In osteoblast cultures, bone nodule formation was visualized by Alizarin Red staining (*G* and *I*) and osteoblastic differentiation by alkaline phosphatase (*ALP*) staining (*H* and *J*). Reduced ALP activity and bone nodule formation in primary osteoblast explant cultures was only detected in HGPS mice (*L*) when compared with wild-type mice (*K*) isolated from animals at the age of 12 weeks. Scale bars: 50 μm.

These observations indicated that the early expression of the HGPS mutation does not cause disturbances in osteoblast differentiation, while the expression of the HGPS mutation over longer periods had a negative effect on the potential of the cells to secrete bone matrix.

To further investigate the detected mineralization defect and fracture-prone nature of HGPS mice, we analyzed the expression of several bone biomarkers. Consistent with the findings of reduced number of bone forming cells, quantitative RT-PCR confirmed that there was a significant reduction of Collagen type 1 (Col1a1), and the osteoblast markers Alkaline phosphatase (Alp) and Osteocalcin (Ocn) in samples from long bones (Fig. 6*A*). In addition, osteoblast-specific runt-related transcription factor 2 (Runx2) and bone biomarkers specific for osteocytes (Phex, Mepe) and osteoclasts (Mmp9) were not significantly reduced compared with wild-type control animals but showed a tendency toward lower expression (Fig. 6*A*).

The Impact of Bone-specific Progerin Expression on DNA Damage Response—To test for changes in Wnt signaling, which has previously been seen in HGPS, we found that the lymphoid enhancer-binding factor (Lef1), which is a Wnt-regulated transcription factor known to regulate osteoblast maturation (35), was significantly reduced in our mouse model. Furthermore, when HGPS mice were compared with wild-type animals, we saw an overall trend toward the lower expression for most of the studied target genes, including Cdkn1a, Jag1, Jag2, Hes1, and Tcf3 (Fig. 6*B*). In accordance with the description of bone disease in HGPS patients, we found no histological signs of skeletal arthritis in our mouse model. However, the fracture prone nature of the skeletal apparatus is very likely to show an inflammatory reaction due to tissue damage signaling. S100 proteins belong to the superfamily of calcium binding proteins and are involved in damage associated molecular patterns (36). Among the S100 proteins, S100A8, S100A9, and S100A4 have been shown to be associated with osteoblast differentiation, and S100A4 has been shown to be a negative regulator for bone mineralization (37–39). We performed expression analysis and found a trend toward higher levels of S100A8 and S100A9 in HGPS mice compared with control animals, even though not significantly different (Fig. 6*C*), while analyzed markers of the interleukin, interferon, and tumor necrosis factor families did not show any indication of altered expression (Fig. 6*C*). Skeletal abnormalities among progeroid syndromes are also reported for diseases with defects in DNA repair (40). In addition, transgenic mouse models have shown that several proteins involved in the DNA damage response play an important role in bone remodeling (41). To determine whether there was a disturbed DNA damage response in progerin-expressing osteoblasts, we examined DNA double strand breaks by immunofluorescence analysis for γH2AX staining that co-localized with Collagen type 1, which served as an osteoblast marker (Fig. 6*D*). We found a significantly higher percentage of cells with numerous γH2AX foci in osteoblast cells isolated from HGPS mice (44.6 ± S.E. 1.6%) compared with wild-type animals (14.8 ± S.E. 1.1%), implicating progerin-induced DNA damage signaling ($p < 0.001$) (Fig. 6*E*).

DISCUSSION

Although bone and dental tissue abnormalities are commonly seen in children with HGPS, and despite the improved description of the clinical features of bone disease and the oral

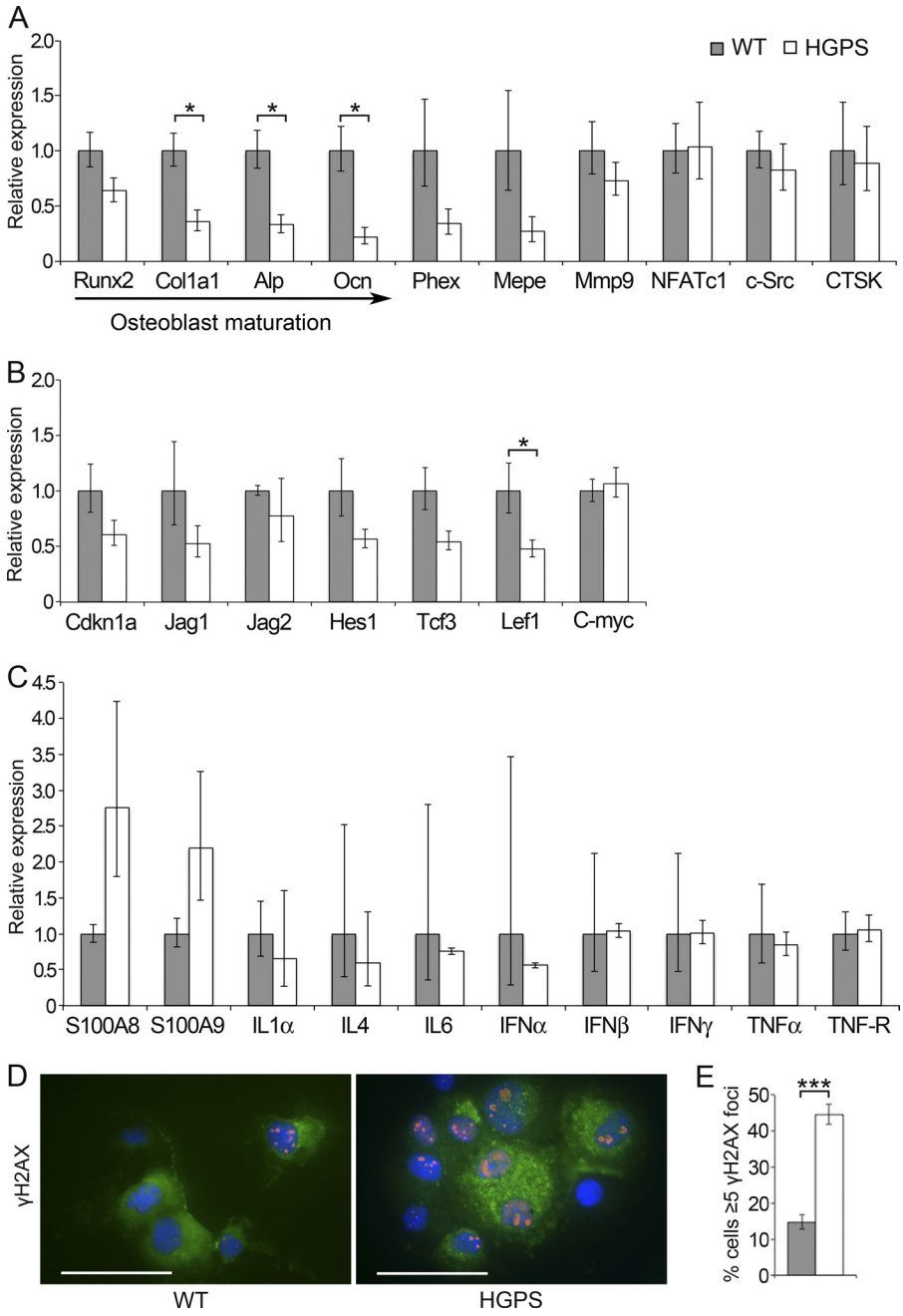

FIGURE 6. **Impaired osteoblast differentiation in HGPS mice leads to down-regulation of bone biomarkers increased DNA damage, elevated inflammatory response and reduced Wnt-mediated Lef1 levels.** Expression levels of osteoblast (Runx2, Cola1a1, Alp, and Ocn), osteocyte (Phex and Mepe), and osteoclast (Mmp9, NFATc1, c-Src, and CTSK) markers in long bones of HGPS and wild-type mice were assessed by relative qPCR. Down-regulation of multiple bone biomarkers and significantly reduced markers specific for osteoblasts (Col1a1, Alp, and Ocn) was observed (*A*). Wnt-mediated Lef1 expression was significantly reduced in HGPS bones, whereas expression levels of genes for the Notch (Cdkn1a, Jag1, Jag2, Hes1) and Wnt (Tcf3, c-Myc) pathways were similar in bone samples from HGPS and control mice (*B*). Expression analysis revealed a trend toward increased levels of the inflammatory response markers S100A8 and S100A9 in bone samples from HGPS mice, while the expression of genes of family members of interleukins (IL1α, IL4, and IL6), interferons (IFNα, IFNβ, and IFNγ) as well as tumor necrosis factors (TNFα, and TNF-R) were unaffected (*C*). Immunofluorescence showed increased numbers of cells with DNA damage in primary osteoblasts that were isolated from HGPS mice (*D*). The frequency of cells with $\geq$5 γH2AX positive foci (*red*) was counted, Collagen type 1 staining was used as an osteoblast marker (*green*), and nuclei were counterstained with DAPI (*blue*) (*D*, *E*). Values represent the mean $\pm$ S.E. (*, $p < 0.05$; ***, $p < 0.001$). Scale bars: 50 μm.

and craniofacial phenotype in HGPS, very little is known about the molecular mechanism underlying the reported skeletal and dental abnormalities (2–5, 42). In this study, we have utilized a tissue-specific approach for the development of a mouse model that allows us to spatially restrict the expression of a target gene to osteoblast cells during development. We took advantage of a previously published Sp7-tTA transactivator mouse (25) to drive the expression of wild-type and mutated human lamin A. Sp7 is a bone specific transcription factor that is active in osteoblastic progenitors and has been shown to be essential for osteoblast differentiation and bone formation (26). Expression analysis, by RT-PCR and Western blot, demonstrated that the transgenic expression in the bone tissue of HGPS mice was tightly regulated by the transactivator system. Immunofluores-

cence staining on primary explant cultures from mouse calvariae confirmed the expression and lamina localization of human lamin A and progerin in osteoblast cells. The analysis of HGPS mice revealed an external phenotype that was already evident at postnatal week 5, which included growth retardation, abnormal gait with striking balance problems, spontaneous bone fractures and kyphosis. The increased detection of callus formation along the costovertebral junction and fracture sites in long bones suggested an altered bone quality. The compromised bone strength was confirmed by the three-point bending test. The bone parameter measurements obtained from the pQCT analysis showed a reduced trabecular BMD together with increased cortical bone thickness. Similar features of abnormalities in BMD, bone structural geometry and skeletal strength have also been found in children with HGPS (5). The brittle bone characteristics in our HGPS mice are also present in mouse models for other skeletal diseases with defective Collagen type 1 secretion, such as many forms of osteogenesis imperfecta (43). Collagen type 1 is the main component of the organic bone matrix, which is secreted by osteoblasts and is essential for proper bone biomineralization. The bone mineral provides mechanical strength and the load bearing characteristic of the skeleton, while the organic matrix provides elasticity, flexibility, and structural organization of the bone (44). Expression analysis showed down-regulation of Collagen type 1 in HGPS mice compared with wild-type mice, indicating a dysfunctional or an abnormal development of osteoblastic cells. Osteoblastogenesis is a complex, tightly regulated process of mesenchymal cell origin where the cell fate, proliferation, and differentiation are regulated by several markers. Runx2 is an important transcription factor that regulates the commitment to the osteogenic lineage and acts upstream of Osterix. Osterix and alkaline phosphatase are early proliferation markers, whereas Osteocalcin is a later marker of bone formation (45). To further examine the mineralization defect in our HGPS mice and to test if it was caused by defective osteoblast differentiation, we performed relative quantification of the expression of osteoblast-specific bone markers. The results showed a significant reduction of alkaline phosphatase and Osteocalcin, which is consistent with the observed loss of bone-forming cells. However, it may also indicate aberrant osteoblast differentiation, detected *in vitro*. Together with our histological observations, the lack of viable osteocytes along with a significant reduction of Wnt-mediated Lef1 (an osteoblast maturation regulator), our findings support a model where impaired osteoblast maturation is a result of expression of the HGPS mutation. Bone quality is, however, secured by permanent bone remodeling. The complex interaction of osteoblastic bone formation and osteoclastic bone resorption, together with osteocytic regulatory and signaling function, is based on the balanced interplay of biochemical and mechanical factors and plays an important role in skeletal structure maintenance (46). Along with the significant reduction of osteoblast-specific bone biomarkers, we also detected a trend of the suppressed expression of analyzed bone markers for osteocytes and osteoclasts (Phex, Mepe, and Mmp9) in our HGPS mice. This suggests that the osteoblast-specific expression of HGPS mutation disturbs the intracellular interaction between osteoblasts, osteoclasts, and osteocytes. The reduced histochemical TRAP staining on long bone sections in HGPS mice is, in accordance with the suppressed expression of osteoclasts bone marker Mmp9, further indicating reduced osteoclast activity. The skeletal abnormalities that we observed in the HGPS mice, including abnormal osteoblast differentiation, loss of bone forming cells, and decreased bone resorption are similar to the findings in lamin A/C-deficient mice and in mice overexpressing unprocessed prelamin A (47, 48). In addition HGPS mice showed common cellular and pathological changes that occur in the aging bone of normal mice, including distorted organization, and a hypocellular bone marrow with prominent white adipocytes (49, 50). This is in agreement with a recent study where they showed that disturbed osteoclast and osteoblast activity disrupted the hematopoietic stem cell niche in the bone marrow (51).

In summary, in this study, we have shown that expression of the HGPS mutation in osteoblasts and osteocytes has a dramatic effect on the structure and function of bone. In addition, we showed that the expression of the HGPS mutation induces a DNA damage response in osteoblasts and possibly inflammation, which results in a bone mineralization defect. The reported HGPS mouse model is a promising system to study bone disease in HGPS because it resembles the phenotype described in affected individuals. The altered osteoblast differentiation and defective bone mineralization indicate general mechanisms that are most likely affecting the bone microenvironment through typical age-related signs, including increased DNA damage signaling. Finally, this is the first study, to our knowledge, to show that expression of the HGPS mutation in the bone results in loss of osteocytes, and disrupted organization of the bone marrow and this model will be useful for testing treatments for HGPS and drugs targeting aging associated diseases.

Acknowledgments—We acknowledge the technical assistance of Hanna Sagelius, Sofia Rodriguez, Tomás McKenna, Léa Maitre, Emma Eriksson, and Carin Lundmark.

REFERENCES

1. DeBusk, F. L. (1972) The Hutchinson-Gilford progeria syndrome. Report of 4 cases and review of the literature. *J. Pediatr.* **80,** 697–724
2. Merideth, M. A., Gordon, L. B., Clauss, S., Sachdev, V., Smith, A. C., Perry, M. B., Brewer, C. C., Zalewski, C., Kim, H. J., Solomon, B., Brooks, B. P., Gerber, L. H., Turner, M. L., Domingo, D. L., Hart, T. C., Graf, J., Reynolds, J. C., Gropman, A., Yanovski, J. A., Gerhard-Herman, M., Collins, F. S., Nabel, E. G., Cannon, R. O., 3rd., Gahl W. A., and Introne W. J. (2008) Phenotype and course of Hutchinson-Gilford progeria syndrome. *N. Engl. J. Med.* **358,** 592–604
3. Gordon, L. B., McCarten, K. M., Giobbie-Hurder, A., Machan, J. T., Campbell, S. E., Berns, S. D., and Kieran, M. W. (2007) Disease progression in Hutchinson-Gilford progeria syndrome: impact on growth and development. *Pediatrics* **120,** 824–833
4. Gardner, D. G., and Majka, M. (1969) The early formation of irregular secondary dentine in progeria. *Oral Surg Oral Med. Oral Pathol.* **28,** 877–884
5. Gordon, C. M., Gordon, L. B., Snyder, B. D., Nazarian, A., Quinn, N., Huh, S., Giobbie-Hurder, A., Neuberg, D., Cleveland, R., Kleinman, M., Miller, D. T., and Kieran, M. W. (2011) Hutchinson-Gilford progeria is a skeletal dysplasia. *J. Bone Miner. Res.* **26,** 1670–1679
6. Baker, P. B., Baba, N., and Boesel, C. P. (1981) Cardiovascular abnormali-

ties in progeria. Case report and review of the literature. *Arch. Pathol. Lab. Med.* **105,** 384–386
7. Shozawa, T., Sageshima, M., and Okada, E. (1984) Progeria with cardiac hypertrophy and review of 12 autopsy cases in the literature. *Acta Pathol. Jpn.* **34,** 797–811
8. De Sandre-Giovannoli, A., Bernard, R., Cau, P., Navarro, C., Amiel, J., Boccaccio, I., Lyonnet, S., Stewart, C. L., Munnich, A., Le Merrer, M., and Lévy, N. (2003) Lamin a truncation in Hutchinson-Gilford progeria. *Science* **300,** 2055
9. Eriksson, M., Brown, W. T., Gordon, L. B., Glynn, M. W., Singer, J., Scott, L., Erdos, M. R., Robbins, C. M., Moses, T. Y., Berglund, P., Dutra, A., Pak, E., Durkin, S., Csoka, A. B., Boehnke, M., Glover, T. W., and Collins, F. S. (2003) Recurrent *de novo* point mutations in lamin A cause Hutchinson-Gilford progeria syndrome. *Nature* **423,** 293–298
10. Fisher, D. Z., Chaudhary, N., and Blobel, G. (1986) cDNA sequencing of nuclear lamins A and C reveals primary and secondary structural homology to intermediate filament proteins. *Proc. Natl. Acad. Sci. U.S.A.* **83,** 6450–6454
11. Burke, B., and Stewart, C. L. (2002) Life at the edge: the nuclear envelope and human disease. *Nat. Rev. Mol. Cell Biol.* **3,** 575–585
12. Lutz, R. J., Trujillo, M. A., Denham, K. S., Wenger, L., and Sinensky M. (1992) Nucleoplasmic localization of prelamin A: implications for prenylation-dependent lamin A assembly into the nuclear lamina. *Proc. Natl. Acad. Sci. U.S.A.* **89,** 3000–3004
13. Sinensky, M., Fantle, K., Trujillo, M., McLain, T., Kupfer, A., and Dalton, M. (1994) The processing pathway of prelamin A. *J. Cell Sci.* **107,** 61–67
14. Pendás, A. M., Zhou, Z., Cadiñanos, J., Freije, J. M., Wang, J., Hultenby, K., Astudillo, A., Wernerson, A., Rodríguez, F., Tryggvason, K., and López-Otín, C. (2002) Defective prelamin A processing and muscular and adipocyte alterations in Zmpste24 metalloproteinase-deficient mice. *Nat. Genet.* **31,** 94–99
15. Bergo, M. O., Gavino, B., Ross, J., Schmidt, W. K., Hong, C., Kendall, L. V., Mohr, A., Meta, M., Genant, H., Jiang, Y., Wisner, E. R., Van Bruggen, N., Carano, R. A., Michaelis, S., Griffey, S. M., and Young, S. G. (2002) Zmpste24 deficiency in mice causes spontaneous bone fractures, muscle weakness, and a prelamin A processing defect. *Proc. Natl. Acad. Sci. U.S.A.* **99,** 13049–13054
16. Goldman, R. D., Shumaker, D. K., Erdos, M. R., Eriksson, M., Goldman, A. E., Gordon, L. B., Gruenbaum, Y., Khuon, S., Mendez, M., Varga, R., and Collins, F. S. (2004) Accumulation of mutant lamin A causes progressive changes in nuclear architecture in Hutchinson-Gilford progeria syndrome. *Proc. Natl. Acad. Sci. U.S.A.* **101,** 8963–8968
17. Dechat, T., Shimi, T., Adam, S. A., Rusinol, A. E., Andres, D. A., Spielmann, H. P., Sinensky, M. S., and Goldman, R. D. (2007) Alterations in mitosis and cell cycle progression caused by a mutant lamin A known to accelerate human aging. *Proc. Natl. Acad. Sci. U.S.A.* **104,** 4955–4960
18. Cao, K., Capell, B. C., Erdos, M. R., Djabali, K., and Collins, F. S. (2007) A lamin A protein isoform overexpressed in Hutchinson-Gilford progeria syndrome interferes with mitosis in progeria and normal cells. *Proc. Natl. Acad. Sci. U.S.A.* **104,** 4949–4954
19. Sullivan, T., Escalante-Alcalde, D., Bhatt, H., Anver, M., Bhat, N., Nagashima, K., Stewart, C. L., and Burke, B. (1999) Loss of A-type lamin expression compromises nuclear envelope integrity leading to muscular dystrophy. *J. Cell Biol.* **147,** 913–920
20. Mounkes, L. C., Kozlov, S., Hernandez, L., Sullivan, T., and Stewart, C. L. (2003) A progeroid syndrome in mice is caused by defects in A-type lamins. *Nature* **423,** 298–301
21. Yang, S. H., Meta, M., Qiao, X., Frost, D., Bauch, J., Coffinier, C., Majumdar, S., Bergo, M. O., Young, S. G., and Fong, L. G. (2006) A farnesyltransferase inhibitor improves disease phenotypes in mice with a Hutchinson-Gilford progeria syndrome mutation. *J. Clin. Invest.* **116,** 2115–2121
22. de Carlos, F., Varela, I., Germanà, A., Montalbano, G., Freije, J. M., Vega, J. A., López-Otin, C., and Cobo, J. M. (2008) Microcephalia with mandibular and dental dysplasia in adult Zmpste24-deficient mice. *J. Anat.* **213,** 509–519
23. Gossen, M., and Bujard, H. (1992) Tight control of gene expression in mammalian cells by tetracycline-responsive promoters. *Proc. Natl. Acad. Sci. U.S.A.* **89,** 5547–5551
24. Sagelius, H., Rosengardten, Y., Hanif, M., Erdos, M. R., Rozell, B., Collins, F. S., and Eriksson, M. (2008) Targeted transgenic expression of the mutation causing Hutchinson-Gilford progeria syndrome leads to proliferative and degenerative epidermal disease. *J. Cell Sci.* **121,** 969–978
25. Rodda, S. J., and McMahon, A. (2006) Distinct roles for Hedgehog and canonical Wnt signaling in specification, differentiation and maintenance of osteoblast progenitors. *Development* **133,** 3231–3244
26. Nakashima, K., Zhou, X., Kunkel, G., Zhang, Z., Deng, J. M., Behringer, R. R., and de Crombrugghe, B. (2002) The novel zinc finger-containing transcription factor osterix is required for osteoblast differentiation and bone formation. *Cell* **108,** 17–29
27. Heinrichs, C., Yanovski, J. A., Roth, A. H., Yu, Y. M., Domené, H. M., Yano, K., Cutler, G. B. Jr., and Baron, J. (1994) Dexamethasone increases growth hormone receptor messenger ribonucleic acid levels in liver and growth plate. *Endocrinology* **135,** 1113–1118
28. Rosengardten, Y., McKenna, T., Grochová, D., and Eriksson, M. (2011) Stem cell depletion in Hutchinson-Gilford progeria syndrome. *Aging Cell* **10,** 1011–1020
29. Nagy, A., Gertsenstein, M., Vintersten, M., and Behringer, R. (2003) Manipulating the Mouse Embryo: A laboratory mannual, 3rd Ed., Cold Spring Harbor Laboratory, Cold Spring Harbor, NY
30. Windahl, S. H., Vidal, O., and Andersson, G. (1999) Increased cortical bone mineral content but unchanged trabecular bone mineral density in female ERβ(−/−) mice. *J. Clin. Invest.* **104,** 895–901
31. Jämsä, T., Tuukkanen, J., and Jalovaara, P. (1998) Femoral neck strength of mouse in two loading configurations: method evaluation and fracture characteristics. *J. Biomech.* **31,** 723–729
32. Jämsä, T., Koivukangas, A., Ryhänen, J., Jalovaara, P., and Tuukkanen, J. (1999) Femoral neck is a sensitive indicator of bone loss in immobilized hind limb of mouse. *J. Bone Miner. Res.* **14,** 1708–1713
33. Schmittgen, T. D., and Livak, K. J. (2008) Analyzing real-time PCR data by the comparative C(T) method. *Nat. Protoc.* **3,** 1101–1108
34. Schmidt, E., and Eriksson, M. (2011) A previously functional tetracycline-regulated transactivator fails to target gene expression to the bone. *BMC Res. Notes* **4,** 282
35. Noh, T., Gabet, Y., Cogan, J., Shi, Y., Tank, A., Sasaki, T., Criswell, B., Dixon, A., Lee, C., Tam, J., Kohler, T., Segev, E., Kockeritz, L., Woodgett, J., Müller, R., Chai, Y., Smith, E., Bab, I., and Frenkel, B. (2009) Lef1 haploinsufficient mice display a low turnover and low bone mass phenotype in a gender- and age-specific manner. *PLoS One* **4,** e5438
36. Foell, D., Wittkowski, H., and Roth, J. (2007) Mechanisms of disease: a 'DAMP' view of inflammatory arthritis. *Nat. Clin. Pract. Rheumatol.* **3,** 382–390
37. Duarte, W. R., Shibata, T., Takenaga, K., Takahashi, E., Kubota, K., Ohya, K., Ishikawa, I., Yamauchi, M., and Kasugai, S. (2003) S100A4: a novel negative regulator of mineralization and osteoblast differentiation. *J. Bone Miner. Res.* **18,** 493–501
38. Zreiqat, H., Howlett, C. R., Gronthos, S., Hume, D., and Geczy, C. L. (2007) S100A8/S100A9 and their association with cartilage and bone. *J. Mol. Histol.* **38,** 381–391
39. Grevers, L. C., de Vries, T. J., Vogl, T., Abdollahi-Roodsaz, S., Sloetjes, A. W., Leenen, P. J., Roth, J., Everts, V., van den Berg, W. B., and van Lent, P. L. (2011) S100A8 enhances osteoclastic bone resorption in vitro through activation of Toll-like receptor 4: implications for bone destruction in murine antigen-induced arthritis. *Arthritis Rheum.* **63,** 1365–1375
40. Cunningham, V. J., D'Apice, M. R., Licata, N., Novelli, G., and Cundy, T. (2010) Skeletal phenotype of mandibuloacral dysplasia associated with mutations in ZMPSTE24. *Bone* **47,** 591–597
41. Wang, X., Goh, C. H., and Li, B. (2007) p38 mitogen-activated protein kinase regulates osteoblast differentiation through osterix. *Endocrinology* **148,** 1629–1637
42. Domingo, D. L., Trujillo, M. I., Council, S. E., Merideth, M. A., Gordon, L. B., Wu, T., Introne, W. J., Gahl, W. A., and Hart, T. C. (2009) Hutchinson-Gilford progeria syndrome: oral and craniofacial phenotypes. *Oral Dis.* **15,** 187–195
43. Kamoun-Goldrat, A. S., and Le Merrer, M. F. (2007) Animal models of osteogenesis imperfecta and related syndromes. *J. Bone Miner. Metab.* **25,** 211–218
44. Robey, P. G., and Boskey, A. L. (2006) in *Primer on the Metabolic Bone*

Disease and Disorders of Mineral Metabolism (Favus, M. J., ed) pp. 12–19, 6th Ed., American Society for Bone and Mineral Research, Durham, NC.
45. Aubin, J. E. (2001) Regulation of osteoblast formation and function. *Rev. Endocr. Metab. Disord.* **2,** 81–94
46. Sims, N. A., and Gooi, J. H. (2008) Bone remodeling: Multiple cellular interactions required for coupling of bone formation and resorption. *Semin. Cell Dev. Biol.* **19,** 444–451
47. Li, W., Yeo, L. S., Vidal, C., McCorquodale, T., Herrmann, M., Fatkin, D., and Duque, G. (2011) Decreased bone formation and osteopenia in lamin a/c-deficient mice. *PLoS One* **6,** e19313
48. Rivas, D., Li, W., Akter, R., Henderson, J. E., and Duque, G. (2009) Accelerated features of age-related bone loss in zmpste24 metalloproteinase-deficient mice. *J. Gerontol. A Biol. Sci. Med. Sci.* **64,** 1015–1024
49. Gimble, J. M., Zvonic, S., Floyd, Z. E., Kassem, M., and Nuttall, M. E. (2006) Playing with bone and fat. *J. Cell Biochem.* **98,** 251–266
50. Rosen, C. J., and Bouxsein, M. L. (2006) Mechanisms of disease: is osteoporosis the obesity of bone? *Nat. Clin. Pract. Rheumatol.* **2,** 35–43
51. Mansour, A., Abou-Ezzi, G., Sitnicka, E., Jacobsen, S. E., Wakkach, A., and Blin-Wakkach, C. (2012) Osteoclasts promote the formation of hematopoietic stem cell niches in the bone marrow. *J. Exp. Med.* **209,** 537–549